Doi: 10.47572/muskutd.1650764

Effect of Benzimidazole Compound on Endoplasmic Reticulum Stress and Unfolded Protein Response (UPR) Signaling Pathway in Hydrogen Peroxide (H_2O_2)-Induced BEAS-2B Cells

Benzimidazol Bileşiğinin Hidrojen Peroksit (H_2O_2) ile Uyarılmış BEAS-2B Hücrelerinde Endoplazmik Retikulum Stresi ve Katlanmamış Protein Yanıtı (UPR) Sinyal Yolakları Üzerindeki Etkisi

Aysel ERASLAN SAKAR[1], Meral URHAN KUCUK[2], Ronak Haj ERSAN[3], Oztekin ALGUL[4]

[1]Hatay Mustafa Kemal University, Faculty of Veterinary Medicine, Department of Genetics, Hatay, Turkey
[2]Hatay Mustafa Kemal University, Faculty of Medicine, Department of Medical Biology, Hatay, Turkey
[3]Cihan University – Duhok, College of Health Sciences, Department of Clinical Biochemistry, Duhok, Iraq
[4]Erzincan Binali Yildirim University, Faculty of Pharmacy, Department of Pharmacy Professional Sciences, Erzincan, Turkey

Öz

Bu çalışmanın birincil amacı, oksidatif stres koşulları altında endoplazmik retikulum stresinin BEAS-2B hücrelerinde mRNA düzeyleri ile protein ekspresyonu üzerindeki etkilerini aydınlatmaktı. İkincil amacı ise, benzimidazol türevi bileşik olan RHE 231'in katlanmamış protein yanıtı sinyal yolağı üzerindeki etkisini değerlendirmekti. Toksik olmayan dozları belirlemek için, hidrojen peroksit (H_2O_2) ve RHE 231 maruziyeti altındaki hücre canlılığı MTT testi ile değerlendirilirken, H2O2'nun neden olduğu hücresel lipid oksidasyonu MDA testi ile ölçüldü. ATF6, PERK, IRE1α ve GRP78 gen ekspresyon düzeylerini analiz etmek için kantitatif gerçek zamanlı PCR kullanıldı, IRE1α ve ATF4 protein düzeyleri ise Western blot yöntemiyle değerlendirildi. Malondialdehit (MDA) seviyeleri, 24 saat sonunda kontrol grubuna kıyasla 10 ve 20 µM konsantrasyonlarında belirgin şekilde daha yüksekti. Benzimidazol türevi bileşik ve H_2O_2 uygulanan gruplarda, kontrol grubuna kıyasla PERK ve IRE1α mRNA düzeylerinde anlamlı artışlar tespit edildi. GRP78 ve ATF6 mRNA ekspresyon düzeylerinde ise herhangi bir grupta kontrol grubuna göre anlamlı bir fark gözlemlenmedi. Western blot analizleri, ATF4 ve IRE1α protein ekspresyonunun, sadece H_2O_2 ve benzimidazol bileşiği ile kombinasyon halinde uygulanan gruplarda kontrol grubuna kıyasla daha yüksek olduğunu ortaya koydu. BEAS-2B hücrelerinde, H_2O_2'ye bağlı oksidatif hasar, ER stresinin aktivasyonuna ve katlanmamış protein yanıt yolağının başlatılmasına yol açtı. Benzimidazol türevi bileşik uygulanan belirli gruplarda protein düzeylerinin azaldığı gözlemlense de, bu azalmanın doz bağımlı bir model sergilemediği gözlendi.

Anahtar Kelimeler: BEAS-2B, Benzimidazol, ER Stresi, Hidrojen Peroksit, Oksidatif Stres

Abstract

The primary objective of this work was to elucidate the impact of endoplasmic reticulum stress on both mRNA level and protein expression on BEAS-2B cells under oxidative stress conditions. The secondary objective was to assess the effect of RHE 231, a benzimidazole compound, on unfolded protein response signaling pathway. To identify non-toxic doses, cell viability under H_2O_2 and RHE 231 exposure was evaluated via the MTT assay, while cellular lipid oxidation due to H_2O_2 was measured using the MDA assay. Quantitative real-time PCR was employed to analyze ATF6, PERK, IRE1α, and GRP78 gene expression levels, while IRE1α and ATF4 protein levels were assessed through western blot method. Malondialdehyde levels were notably higher than the control group at ten and twenty µM concentrations at 24 hours. Significant increases in PERK and IRE1α mRNA levels were detected in the groups in which benzimidazole compound and hydrogen peroxide were applied combined than control group. No significant differences in GRP78 and ATF6 mRNA expression levels were detected in any group relative to the control group. Western blot analysis revealed that ATF4 and IRE1 protein expression was higher in the H_2O_2 alone and combined with benzimidazole compound groups than control group. In BEAS-2B cells, H_2O_2-induced oxidative damage led to the activation of ER stress and launch of the unfolded protein response pathway. Although protein levels diminished in certain groups treated with the benzimidazole compound, it was observed that this decrease did not exhibit a dose-dependent pattern.

Keywords: BEAS-2B, Benzimidazole, ER Stress, Hydrogen Peroxide, Oxidative Stress

Introduction

The endoplasmic reticulum functions as a pivotal cell compartment that ensures the proper folding of both secretory and membrane proteins. Once a protein is correctly folded, it proceed to the Golgi, where it undergoes further modification and is directed to its appropriate cellular locations (1). Disruptions in ER processes—arising from conditions such as oxidative stress, hypoxia, and pathogenic infections—can lead to an imbalance between the ER's capacity and the cellular demand for protein folding, resulting in ER stress (2). ER stress signaling pathways, known as the unfolded protein response (UPR) enhances protein folding and clearance to prevent misfolded protein accumulation, but prolonged ER stress can trigger cell death (3). The UPR is regulated by three ER sensors: IRE1α, ATF6, and PERK. Under normal conditions, their luminal domains are inactive, bound to the ER chaperone GRP78 (BiP). When misfolded proteins accumulate, GRP78 dissociates

	ORCID No
Aysel ERASLAN SAKAR	0000-0002-9230-1622
Meral URHAN KUCUK	0000-0003-1704-1370
Ronak Haj ERSAN	0000-0001-6651-5910
Oztekin ALGUL	0000-0001-5685-7511

Başvuru Tarihi / Received: 04.03.2025
Kabul Tarihi / Accepted : 30.07.2025

Adres / Correspondence : Meral URHAN KUCUK
Hatay Mustafa Kemal University, Faculty of Medicine, Department of Medical Biology, Hatay, Turkey
e-posta / e-mail : meralurhan@hotmail.com

from IRE1, PERK, and ATF6, activating them (4). Specifically, the accumulation of misfolded or unfolded proteins in the respiratory system, causes disruption of lung metabolism. Studies have reported elevated levels of polyubiquitinated proteins in the lung tissue of individuals with chronic obstructive pulmonary disease (COPD).

COPD involves progressive airflow obstruction and emphysema, with high ROS levels detected in the lungs and blood of patients. Proteins that undergo oxidative modification tend to accumulate and aggregate, which can disrupt cellular homeostasis and lead to cell death (5). Nevertheless, the specific genetic and mechanistic pathways underlying COPD pathogenesis remain incompletely understood.

Benzimidazoles, possessing structural similarities to nucleotides, readily interact with biological macromolecules, thereby influencing diverse biological functions and activities. As a notable pharmacophore in medical chemistry, the benzimidazole scaffold confers a highly adaptable heterocyclic structure, enabling a wide range of biological activities (6). Cells synthesize various derivatives, substituting elements such as propylene, fluorine, tetrahydroquinoline, and cyclic compounds, emphasizing the significance of benzimidazoles for their bioavailability and stability.

In this research, an oxidative damage model was established in vitro by exposing human bronchial epithelial cells (BEAS-2B) to hydrogen peroxide (H_2O_2). This study aimed to examine the potential protective role of the RHE 231, benzimidazole derivative compound (1,3-bis(5-chloro-1H-benzo[d]imidazol-2-yl)propane) in mitigating ER stress pathway induced by oxidative stress. Prior works have demonstrated that H_2O_2, an oxidizing agent, induces apoptotic and oxidative damage in BEAS-2B cells (7–8). However, no research has simultaneously examined the ER stress pathway in bronchial epithelial cells under H_2O_2-induced ROS conditions at both protein and gene expression levels. Additionally, the potential protective role of RHE 231 in modulating UPR signaling pathways has yet to be investigated.

Material and Method

Chemical and Reagent

BEAS-2B cell was obtained from the ATCC (Rockville, U.S.A). FBS, penicillin/streptomycin, DMEM, and trypsin/EDTA were sourced from Gibco BRL (Grand Island, U.S.A). β-mercaptoethanol, 2-thiobarbituric Acid (TBA), and H_2O_2 were procured from Merck (U.S.A). RIPA buffer was provided by Santa Cruz Biotechnology (U.S.A). Primary antibodies targeting β-actin and IRE1α were acquired from Thermo Fisher Scientific (U.S.A), while the antibody against ATF4 was obtained from Proteintech Group (U.S.A). Unless otherwise noted, other chemical agents were obtained from Sigma-Aldrich (St. Louis, U.S.A).

Preparation of the Benzimidazole Compound

All chemicals (glutaric acid, 4-chlorobenzene-1,2-diamine) and solvents used in the analysis and synthesis were of spectroscopic or analytic grade (Acros Organics and Sigma-Aldrich) and were used as supplied, without additional purification. The synthesis followed the polyphosphoric acid (PPA) method (9–10). Melting points of the compound were analyzed with a Mettler Toledo melting point system. Infrared spectra were reported using a Perkin-Elmer Spectrum One FT-IR spectrometer, and proton (^1H) and carbon (^{13}C) NMR spectra were acquired using a Bruker 400 MHz spectrometer.

Preparation of Benzimidazole and H_2O_2 Solutions

The benzimidazol compound RHE 231 was dissolved in DMSO and adjusted to final concentrations of 0–2.5–5–10–25–50–75–100 μM in serum-free medium (SF) containing 1% penicillin/streptomycin. Hydrogen peroxide was dissolved in serum-free DMEM containing 1% penicillin/streptomycin to create concentrations of 0–10–20–30–40–50–100–200 μM.

Treatments of Cell Culture

BEAS-2B cells were grown in DMEM containing 10% FBS and 1% penicillin/streptomycin, and were incubated at 37°C in a humidified environment with 5% CO_2. To examine the effect of RHE 231 on H_2O_2-treated cells, cells at 70-80% confluence were first exposed to indicated H_2O_2 concentrations for 1 hour, followed by treatment with RHE 231. After washing with PBS to eliminate extracellular H_2O_2, fresh medium containing the desired RHE 231 concentration was added. The cells were then incubated and collected for subsequent analysis.

Determination of Cell Viability

BEAS-2B cell lines were plated in 24-well plates at a density of 10 000 cells per well and were incubated at 37°C in 5% (v/v) CO_2 humidified incubator. Cell survival was assessed using the MTT assay, which serves as a highly sensitive indicator of cellular metabolic activity. MTT solution was added to the culture medium, and cells were incubated for 1 hour at 37°C in the dark. Following culture medium removal, the formazan crystals were dissolved in 500 μL of DMSO, and absorbance was recorded at 595–670 nm in a microplate spectrophotometer (Multiskan GO, Thermo Scientific).

Measurement of Cellular Lipid Oxidation

Malondialdehyde (MDA) levels were assessed as an indicator of lipid peroxidation, following the

thiobarbituric acid (TBA) assay based on established methods (11). Cells were harvested, washed with chilled PBS, lysed using 2 mL of lysis buffer, and centrifuged at 10,000×*g* for 10 min. The lysate was combined with TBA and incubated at 95°C in a water bath for 30 min, then subsequently cooled in an ice bath. The absorbance was recorded spectrophotometrically at 532 nm using a microplate reader (Multiskan GO (Thermo, USA). The results were saved as nmoll/mg protein, and all experiment was performed in triplicates.

Quantitation of Gene Expression by RT-qPCR

The cells were seeded into 6-well plates (2.5×10^5 cells/well) and subsequently treated for 24 hours both with and without RHE addition. Following treatment, total RNA was extracted using the RNeasy Mini Kit (Qiagen) based on the manufacturer's guidelines. RNA purity was assessed by measuring the absorbance ratio at 260 nm/280 nm on a plate reader (Multiskan GO, Thermo). cDNA synthesis was performed by the Applied Biosystems High-Capacity cDNA Reverse Transcripton Kit (USA). The real-time PCR was carried out with Applied Biosystem Power SYBR Green PCR Master Mix on a Rotor-Gene Q (Qiagen). The primer sequences for GRP78, ATF6, PERK, and IRE1α (12) are presented in Table 1.

Table 1. Primer sets used in the study

Gene	Primer sequences	Literature
PERK	F: 5'-TGTCGCCAATGGGATAGTGACGAA- R: 5'-AATCCGGCTCTCGTTTCCATGTCT-3	12
ATF6	F: 5'-ATGTCTCCCCTTTCCTTATATGGT-3' R: 5'-AAGGCTTGGGCTGAATTGAA-3'	12
IRE1α	F: 5'-GGGAAATACTCTACCAGCCT-3' R: 5'-GAAATCTCTCCAGCATCTTG-3'	12
GRP78	F: 5'-CAACCCCGAGAACACGGTC-3' R: 5'-CTGCACAGACGGGTCATTC-3'	12

Beta-actin was used as a housekeeping gene (Qiagen, Germany). Each RT-qPCR reaction was performed in a 25 µL volume containing 100 ng of cDNA, 100 nM primer, Master Mix, and nuclease-free water. Cycling parameters included an initial denaturation step of 10 minutes at 95°C, followed by 40 cycles of 15 sec at 95°C and annealing for 60 sec at 60°C. A melting curve confirmed single amplicon formation. The fold change in gene expression was calculated by the formula $2^{\Delta\Delta}$CT (13), following normalization to β-actin.

Western Blot Analysis

To quantify protein levels, Western blotting was performed. Cells were rinsed with PBS, scraped off, and lysed on ice using RIPA buffer (Santa Cruz Biotechnology) containing sodium orthovanadate, PMSF, and protease inhibitors. The homogenate was centrifuged at 10,000×*g* for 10 minutes at 4°C, and total protein content was detected using the BCA assay (Pierce, USA) and BSA as a standard. 50 µg protein was separated on a SDS-PAGE gel and transferred to a PVDF membrane by electroblotting. To prevent non-specific binding, the membranes were incubated with 5% (w/v) skim milk powder in TBST for 1 h at room temperature. They were then incubated overnight with primary antibodies targeting ATF4, IRE1α, and β-actin (Thermo-Fisher Scientific and Proteintech), followed by incubation with an HRP-conjugated secondary antibody. The protein bands were visualized using an ECL kit (Bio-Rad), and captured with a ChemiDoc imaging system. Band intensities were assessed using Image Lab software (Bio-Rad).

Statistical Analysis

The SPSS 23 software was used for statistical evaluations (IBM Corporation, Armonk, NY). For the MDA analysis, the Mann-Whitney test was used to compare the groups. Data were declared as mean ± SD and those with $p<0.05$ were considered statistically significant. For the gene and protein expression analysis, a one-way ANOVA followed by post hoc Dunnett's test was performed using GraphPad Prism 10 (GraphPad, CA, USA).

Results

Synthesis of the Benzimdazole Compound

A solution containing 4-chlorobenzene-1,2-diamine (2 mmol) and glutaric acid (1 mmol) was heated in polyphosphoric acid (PPA) at 120°C for 1 hour, then further stirred at 180°C for an additional 12 hours. The progress of the reaction was monitored via thin-layer chromatography (TLC), with ultraviolet (UV) light used to visualize the spots on TLC plates (Kieselgel 60 F254, ready-to-use aluminum plate coated with 0.2 mm thickness). The reaction solution was transferred to ice water, neutralized with 5 M NaOH to a basic pH to induce product precipitation. The obtained precipitate was collected by filtration, washed with cold water, and subsequently recrystallized from an appropriate solvent. The crystalline compound was then filtered and the isolated solid was dried under reduced pressure (Figure 1).

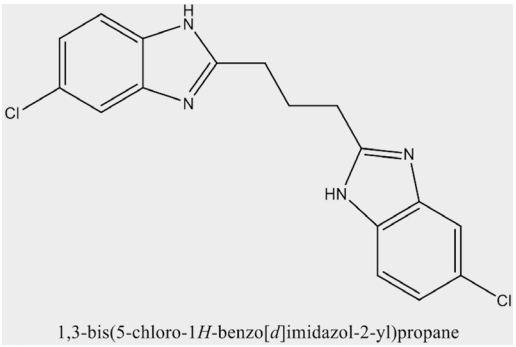

Figure 1. The chemical structure of synthesized benzimidazole compound RHE-231.

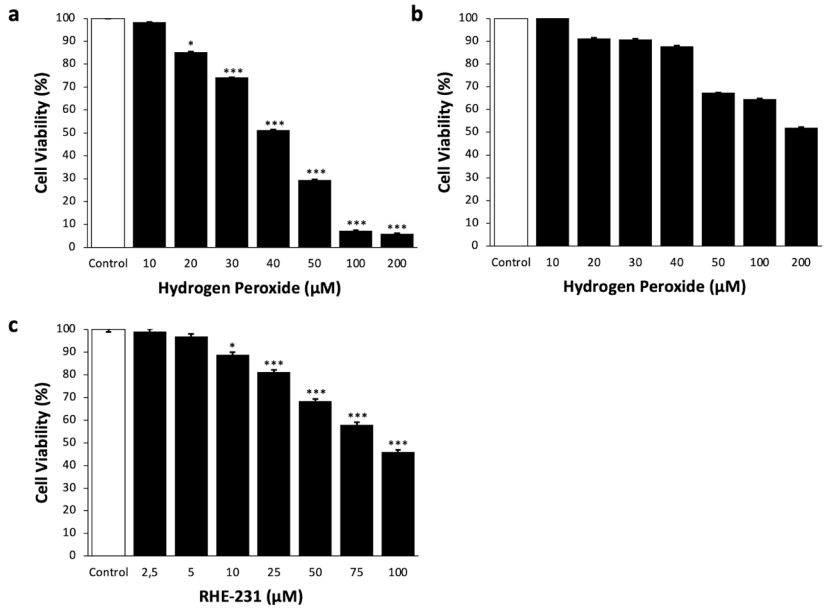

Figure 2. BEAS-2B cell viability after exposure to different concentrations of **a.** H_2O_2 for 24 h, **b.** H_2O_2 for 48 h, and **c.** RHE-231 for 24 h. Cell viability was determined using the MTT assay. The results were obtained from three independent experiments performed in triplicate and were represented as mean ± SD (*p<0.05, ***p<0.001).

Effect on Cell Viability

To evaluate the cytotoxic effects of H_2O_2 on BEAS-2B cell line, they were treated with different concentrations of H_2O_2 (0-200 µM) for 24-hour and 48-hour, and cell viability was measured using the MTT assay. Cell viability was significantly decreased in a concentration-specific manner after 24 hours of H_2O_2 exposure compared to untreated control cells. Significant reductions in cell viability were observed at 20 (p<0.05), as well as at 30, 40, 50, 100, and 200 µM (p<0.001) (Figure 2a). As a result, concentrations of 10 and 20 µM were chosen for the current research. After 48 hours of exposure, no significant alterations in viability were detected at none of applied concentration (Figure 2b). Based on these findings, 10 and 20 µM concentrations of H_2O_2 and a 24-hour exposure duration were chosen for further experiments. Treatment conditions were determined by assessing cell viability after 24-hour treatment with different doses (0-100 µM) of RHE, using the MTT assay. Significant reductions in cell viability were noted at 10 (p<0.05), 25, 50, 75, and 100 µM doses (p<0.001) (Figure 2c).

Effect on Oxidative Stress Induction

Oxidant-induced cellular injury leads to lipid peroxidation. MDA levels, indicative of lipid peroxidation, were measured to assess oxidative damage. Following 24-hour exposure to H_2O_2 at 10 and 20 µM, a concentration-specific increase in MDA levels was detected in the cells, showing a highly significant rise compared to the control (p<0.001 at both concentrations) (Figure 3). Specifically, the MDA concentration reached 0.54±0.17 for 10 µM and 1.02±0.63 for 20 µM, indicating a correlation between oxidative stress and H_2O_2 levels.

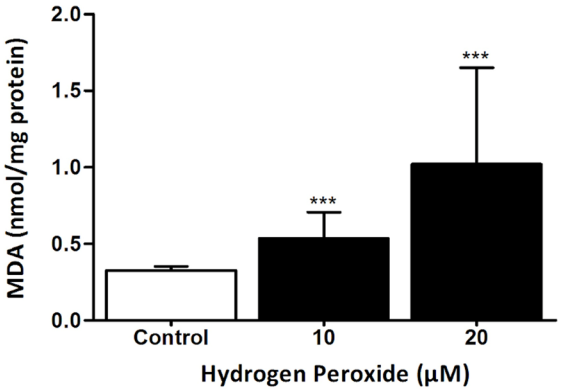

Figure 3. Oxidative damage in BEAS-2B cells after exposure to H_2O_2 for 24 h. Data were expressed as mean±SD from three independent experiments. ***p<0.001 compared with control.

Effect on Expression Levels of ER Stress Genes

Oxidative stress interferes with protein folding in the endoplasmic reticulum, activating the unfolded protein response (UPR) and causing ER stress (5). This study investigated whether exposure to H_2O_2 triggers ER stress and if RHE 231 can alleviate this stress level by examining the mRNA of GRP78, ATF6, PERK, and IRE1α in BEAS-2B cell line. The cells were treated for 24 hours with 10 µM H_2O_2+10 µM RHE 231, 10 µM H_2O_2+5 µM RHE 231, 10 µM H_2O_2, 20 µM H_2O_2+10 µM RHE 231, 20 µM H_2O_2+5 µM RHE 231, and 20 µM H_2O_2. RT-qPCR analysis revealed no meaningful alterations in the transcript amounts of GRP78, ATF6, PEPK, and IRE1α in the 10 µM H_2O_2, 20 µM H_2O_2, 10 µM H_2O_2+10 µM RHE 231, and 10 µM H_2O_2+5 µM RHE 231 groups against the control group.

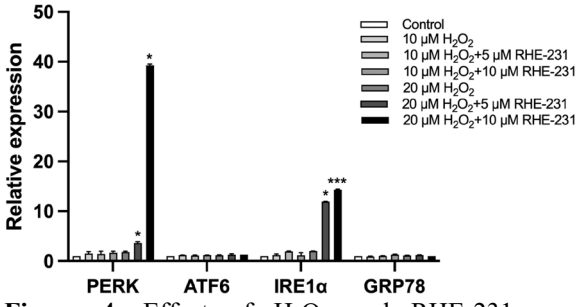

Figure 4. Effect of H_2O_2 and RHE-231 on endoplasmic reticulum (ER) stress-related gene expression. BEAS-2B cells were treated with the indicated concentrations of H_2O_2 and RHE-231 for 24 h. The bar graph showed the fold change after normalization according to β-actin mRNA expression of PERK, ATF6, IRE1α, and GRP78. Data were normalized against β-actin mRNA levels. *p<0.05 and ***p<0.001. All data shown are representative of three biological replicates.

However, there was a notable increase in PERK and IRE1α expressions in the 20 μM H_2O_2+10 μM RHE 231 and 20 μM H_2O_2+5 μM RHE 231 groups relative to control (Figure 4). In the 20 μM H_2O_2+5 μM RHE 231 group, IRE1α gene expression increased by 11.95-fold (p<0.05), while PERK expression rose by 3.65-fold (p<0.05). Similarly, in the 20 μM H_2O_2+10 μM RHE 231 group, IRE1α expression showed a 14.31-fold increase (p<0.001), whereas PERK expression surged 39.27-fold. There were no notable differences in GRP78 and ATF6 expression in any group compared to the controls.

Effect on Immunoblot of ER Stress Proteins

To gain deeper insight into how RHE 231 may defend BEAS-2B cells against oxidative stress, IRE1α and ATF4 expression levels were analyzed using immunoblotting. Immunofluorescence staining indicated dose-dependent increases in UPR markers ATF4 and IRE1α in BEAS-2B cells exposed to H_2O_2. As illustrated in Figure 5, there were notable increases in ATF4 (Figure 5a) and IRE1α (Figure 5b) in the 20 μM H_2O_2+10 μM RHE 231, 20 μM H_2O_2+5 μM RHE 231, and 20 μM H_2O_2 groups relative to the controls (p<0.001).

Taken together, these results indicate that H_2O_2 triggers endoplasmic reticulum stress by disrupting endoplasmic reticulum homeostasis in BEAS-2B cell line in a dose-related manner. Moreover, protein expression decreased in certain samples treated with the benzimidazole compound, though this was not dependent on concentration.

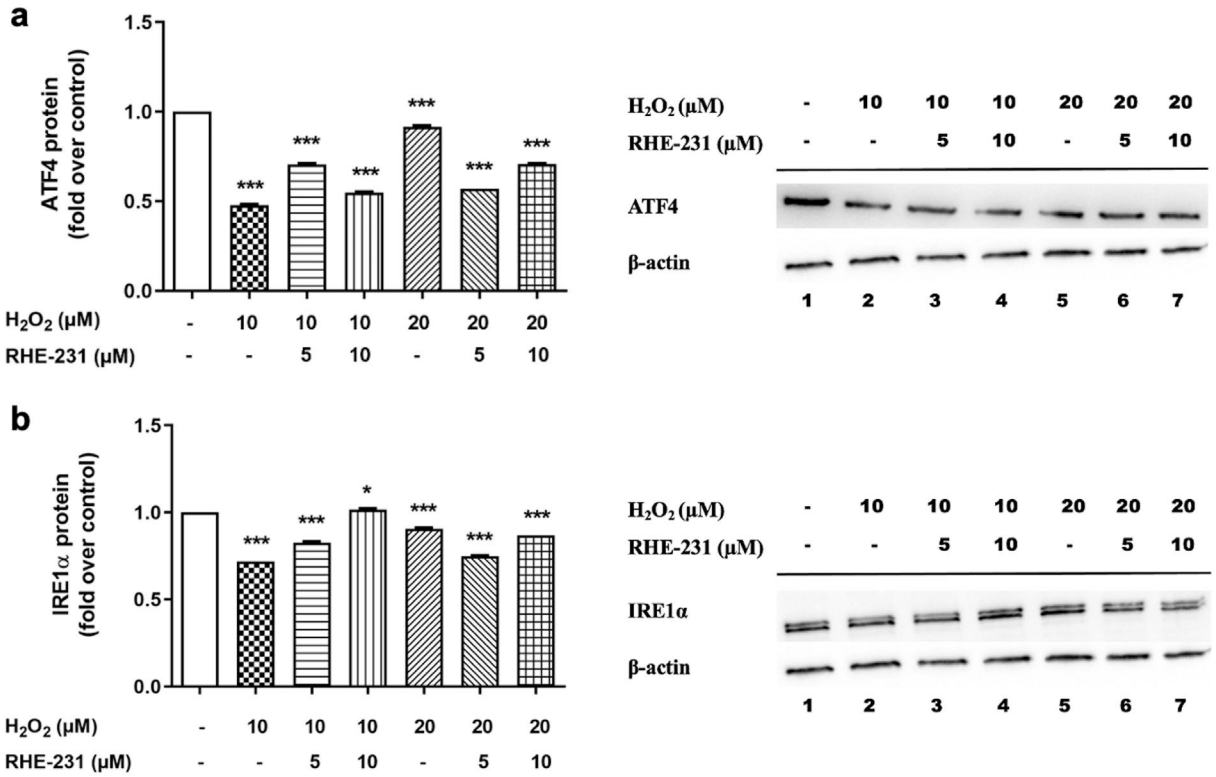

Figure 5. Western blotting analysis of ATF4 (**a**) and IRE1α (**b**) after treatment with H_2O_2 and RHE-231 for the indicated concentrations for 24 h. The band intensities were reported as a fold over the control after normalization with the β-actin loading reference. *p<0.05 and ***p<0.001. All data shown are representative of three biological replicates.

Discussion

BEAS-2B cells are commonly used in research on bronchial conditions (14). Numerous studies have demonstrated that hydrogen peroxide (H_2O_2), a pro-oxidant present in tobacco, causes oxidative stress and apoptosis in bronchial cell lines (7–8). This study investigated which endoplasmic reticulum stress pathway stimulates the UPR and whether a benzimidazole compound alleviates ER stress signaling under oxidative stress state in BEAS-2B cells. With this objective, the cells were treated with H_2O_2, and the MTT assay was employed to determine the optimal concentration. The results indicated no significant decrease in cell viability at 10 µM H_2O_2 after 24 hours, while higher concentrations (20–200 µM) led to a significant reduction ($p<0.001$ for 30 µM and above and $p<0.05$ for 20 µM). After 48 hours, cell viability showed no considerable difference at any dose level than control ($p>0.05$).

Hydrogen peroxide is commonly used to investigate cellular damage caused by oxidative stress in numerous experimental models, such as tissue and cell cultures (15). Tsao et al. (16) evaluated the protective effects of triterpenic acids in 16HBE and BEAS-2B cells exposed to 100 µM H_2O_2, finding a significant decrease in cell viability and increased DNA breakage in both cell types.

Oxidative cell stress triggers lipid peroxidation, wherein ROS target PFAs in cellular membranes, initiating a self-perpetuating chain reaction leading to aldehyde production. This degrades membrane lipids, causing cellular injury (17). In the current study, oxidative damage in H_2O_2-treated cells was assessed by measuring malondialdehyde (MDA) levels. BEAS-2B cells exposed to H_2O_2 at 20 and 10 µM for 24 hours exhibited significantly elevated MDA levels against the control ($p<0.001$ for both concentrations). Some researchers exposed BES-2B cells to PM2.5 for 24 hours, finding significantly higher levels of MDA and ROS compared to controls ($p<0.01$) (18).

Benzimidazole comprises a fused structure of benzene and imidazole rings and represents a bioactive heterocyclic compound with various pharmacological effects, including antimicrobial (19), anti-inflammatory (20), antidiabetic (21), and antioxidant (22) activities. To assess the protective effects of RHE 231 on H_2O_2-induced ER stress signaling, cell viability was evaluated across RHE 231 concentrations (0–100 µM) over a 24-hour period. Results indicated no significant effect on cell viability rate at 5 µM ($p>0.05$), whereas cell viability declined significantly at 100, 75, 50, 25 ($p<0.001$), and 10 µM ($p<0.05$) against the control. Researchers synthesized 14 benzimidazole derivatives and assessed their cytotoxicity in BEAS-2B and A549 cells, finding three with strong antimicrobial activity (23). A group of researchers studied a novel benzimidazole derivative with melatonin-like properties *in vitro*, showing its antioxidant effects in the EMLP system by inhibiting EMLP at 0.5 mM, likely via interactions with apolar phospholipids (24). Kerimov et al. (25) synthesized benzimidazole derivatives with thiadiazoylmethylbenzimidazole, thiosemicarbazide, and triazoylmethylbenzimidazole, finding that the thiosemicarbazide derivative inhibited lipid peroxidation by 80–100%.

Oxidative stress disrupts ER protein folding, and when unfolded proteins exceed the ER's capacity, it activates the UPR (26). UPR branches (IRE1, PERK, ATF6) regulate transcription, translation, and post-translational events to mitigate stress. If persistent, ER stress can induce programmed cell death. In this study, PERK and IRE1α expression, key UPR components, increased in the treatment group than control group. Notably, a marked rise in gene expression was observed in the 20 µM H_2O_2+10 µM RHE-231 and 20 µM H_2O_2+5 µM RHE-231 groups against the control group. The PERK gene expression increased 3.65-fold ($p<0.05$), and IRE1α increased 11.95-fold ($p<0.05$) in the 20 µM H_2O_2+5 µM RHE-231 group. In the 20 µM H_2O_2+10 µM RHE-231 group, IRE1α expression increased 14.31-fold ($p<0.001$), while PERK expression rose 39.27-fold ($p<0.05$). However, GRP78 and ATF6 expression levels showed no significant differences among all the groups. To strengthen the gene expression findings, we assessed protein expression levels. Significant increases in IRE1α and ATF4 protein levels were observed in the 20 µM H_2O_2+10 µM RHE-231, 20 µM H_2O_2+5 µM RHE-231, and 20 µM H_2O_2 groups than the control group ($p<0.001$). Zhang and Wang (27) examined TUDCA's efficacy in reducing ER stress by exposing neonatal rat cardiomyocytes to H_2O_2 (2–0.1 mM, 6h). Unlike this study, they found H_2O_2 significantly increased GRP78 expression ($p<0.05$), while TUDCA mitigated this effect. IRE1α is an ER stress sensor that, upon activation, splices XBP1 mRNA to produce XBP1s, a transcription factor that promotes ER chaperone expression, cytokine-related genes, protein folding, ERAD, cholesterol synthesis, and ER membrane expansion (28,29,30). The increased IRE1α expression observed in this study indicates its potential role in UPR activation by enhancing ERAD genes, ER chaperones, and ER membrane lipid production. IRE1α gene expression was higher in the 20 µM H_2O_2+5 µM RHE-231 and 20 µM H_2O_2+10 µM RHE-231 groups compared to the 20 µM H_2O_2 group. This indicates that RHE 231 does not relieve ER stress, as IRE1α gene expression did not decrease. These findings are supported by IRE1α protein expression data. Researchers (31) investigated IRE1α, PERK, and ATF6 signaling in HEK293 cells, reporting that each UPR branch displayed different deactivation timelines despite ongoing stress, with IRE1 signaling attenuating first,

followed by ATF6, and finally PERK. Ge et al. (32) investigated the connection between neuropathic pain and ER stress in an SNL rat model. They found that SNL triggered oxidative stress (p>0.05) and significantly activated ER stress markers. TUDCA administration reduced ER stress marker expression and alleviated SNL-induced nociceptive behavior. The PERK cascade plays a vital function in the cellular defense against redox imbalance by promoting the activation of leu zipper (bZIP) domain transcription factor family, especially ATF4 and Nrf2 (33–34). In this study, the observed increase in PERK gene expression with rising H_2O_2 concentrations suggests a protective mechanism against oxidative damage induced by H_2O_2. The results indicate that RHE 231 did not exert a mitigating impact on endoplasmic reticulum stress, as there was no reduction in PERK gene expression. Additionally, the increased protein amounts of ATF4 sitimulated by PERK are consistent with the PERK expression data. Some researchers (35) exposed BEAS-2B cells to diesel exhaust particulate (DEP) and found that ATF4 gene expression level elevated in a time- and dose- dependent pattern. NAC treatment reduced ATF4 expression after DEP exposure, consistent with our findings.

Yu et al. (36) investigated the ER stress-inducing effects of cigarette smoke extract in BEAS-2B cells by measuring p-eIF2α, GRP78, and CHOP expression. They found a time-dependent increase in these markers, while 14,15-EET treatment significantly reduced their expression. Kenche et al. (37) showed that cigarette smoke exposure in mice increased CHOP, p-eIF2α, and p50 ATF6N protein expression. While XBP1s mRNA levels rose slightly after acute exposure, they declined within 12 hours. Other researchers (38) treated with mice to smoke extract for 4 weeks, increasing CHOP and ATF4 levels in lung tissue, which dropped below baseline after a year. CHOP and ATF4 also rose in alveolar macrophage cells after ten days, indicating a dynamic, temporary, and cell-type specific UPR response. Other researchers (39) found that UPR markers (XBP1s, GRP78, ATF6N, CHOP) were undetectable in end-stage COPD lungs but upregulated in pulmonary fibrosis patients and their alveolar epithelial cells.

Conclusion

In our study, H_2O_2 exposure decreased cell viability and elevated lipid peroxidation in BEAS-2B cell line. Oxidative stress, in a dose-dependent manner, induced endoplasmic reticulum stress markers at both protein and gene levels, leading to UPR pathway activation. These results suggest that oxidants like H_2O_2 may play a role in the development of chronic respiratory diseases, particularly COPD. While RHE 231 testing revealed reduced protein expression in certain samples, this reduction did not correlate consistently with concentration.

Acknowledgements

Meral Urhan Kucuk and Aysel Eraslan Sakar have carried out the design and coordinated the study as well as they have checked the last revisions and send the manuscript. The author of the PhD thesis Aysel Eraslan Sakar has carried out the experimental analysis and prepared the manuscript. Oztekin Algul and Ronak Haj Ersan have designed benzimidazole compound.

Conflict of interest statement

The authors declare that there is no conflict of interest.

Ethics Committee Approval: This article does not contain any studies involving animals or human participants performed by any of the authors.

Funding: This work was supported by Hatay Mustafa Kemal University Scientific Research Projects Coordination Unit (Grant number: 16800), Hatay, Turkey.

References

1. Smith MH, Ploegh HL, Weissman JS. Road to ruin: targeting proteins for degradation in the endoplasmic reticulum. Science. 2011;334(6059):1086-90.
2. Aghaei M, Dastghaib S, Aftabi S, et al. The ER Stress/UPR Axis in Chronic Obstructive Pulmonary Disease and Idiopathic Pulmonary Fibrosis. Life (Basel). 2020;11(1).1.
3. Yang M, Kuang M, Wang G, et al. Choline attenuates heat stress-induced oxidative injury and apoptosis in bovine mammary epithelial cells by modulating PERK/Nrf-2 signaling pathway. Mol Immunol. 2021;135:388-97.
4. Li Y, Lu L, Zhang G, et al. The role and therapeutic implication of endoplasmic reticulum stress in inflammatory cancer transformation. Am J Cancer Res. 2022;12(5):2277-92.
5. Fan T, Huang Z, Wang W, et al. Proteasome inhibition promotes autophagy and protects from endoplasmic reticulum stress in rat alveolar macrophages exposed to hypoxia-reoxygenation injury. J Cell Physiol. 2018;233(10):6748-58.
6. Narasimhan B, Sharma D, Kumar P. Benzimidazole: a medicinally important heterocyclic moiety. Med Chem Res. 2012;21(3):269-83.
7. Xue X, Piao JH, Nakajima A, et al. Tumor necrosis factor alpha (TNFalpha) induces the unfolded protein response (UPR) in a reactive oxygen species (ROS)-dependent fashion, and the UPR counteracts ROS accumulation by TNFalpha. J Biol Chem. 2005;280(40):33917-25.
8. Gao X, Fu L, Xiao M, et al. The nephroprotective effect of tauroursodeoxycholic acid on ischaemia/reperfusion-induced acute kidney injury by inhibiting endoplasmic reticulum stress. Basic Clin Pharmacol Toxicol. 2012;111(1):14-23.
9. Algul O, Duran N. Activity of bisbenzimidazoles derivatives to Staphylococcus epidermidis. Asian J Chem. 2007;19(4):31-45.
10. Ersan RH, Bolelli K, Gonca S, et al. Bisbenzimidazole derivatives as potential antimicrobial agents: Design, synthesis, biological evaluation and pharmacophore analysis. Pharm Chem J. 2021;55(2):149-58.

11. Ohkawa H, Ohishi N, Yagi K. Assay for lipid peroxides in animal tissues by thiobarbituric acid reaction. Anal Biochem. 1979;95(2):351-8.
12. Chou CK, Liu W, Hong YJ, et al. Ethyl Acetate Extract of Scindapsus cf. hederaceus Exerts the Inhibitory Bioactivity on Human Non-Small Cell Lung Cancer Cells through Modulating ER Stress. Int J Mol Sci. 2018;19(7).
13. Livak KJ, Schmittgen TD. Analysis of relative gene expression data using real-time quantitative PCR and the 2(-Delta Delta C(T)) Method. Methods. 2001;25(4):402-8.
14. Yu C, Zhang L. Methylprednisolone up-regulates annexin A1 (ANXA1) to inhibit the inflammation, apoptosis and oxidative stress of cigarette smoke extract (CSE)-induced bronchial epithelial cells, a chronic obstructive pulmonary disease in vitro model, through the formyl peptide receptor 2 (FPR2) receptors and the adenosine 5'-monophosphate (AMP)-activated protein kinase (AMPK) pathway. Bioengineered. 2022;13(2):4028-38.
15. Thannickal VJ, Fanburg BL. Reactive oxygen species in cell signaling. Am J Physiol Lung Cell Mol Physiol. 2000;279(6):L1005-28.
16. Tsao SM, Yin MC. Antioxidative and antiinflammatory activities of asiatic acid, glycyrrhizic acid, and oleanolic acid in human bronchial epithelial cells. J Agric Food Chem. 2015;63(12):3196-204.
17. La Maestra S, De Flora S, Micale RT. Effect of cigarette smoke on DNA damage, oxidative stress, and morphological alterations in mouse testis and spermatozoa. Int J Hyg Environ Health. 2015;218(1):117-22.
18. Wu J, Shi Y, Asweto CO, et al. Fine particle matters induce DNA damage and G2/M cell cycle arrest in human bronchial epithelial BEAS-2B cells. Environ Sci Pollut Res Int. 2017;24(32):25071-81.
19. Eisa HM, Barghash AEM, Badr SM, et al. Synthesis and antimicrobial activity of certain benzimidazole and fused benzimidazole derivatives. Indian J Chem. 2010;49B:1515-25.
20. Gaba M, Singh D, Singh S, et al. Synthesis and pharmacological evaluation of novel 5-substituted-1-(phenylsulfonyl)-2-methylbenzimidazole derivatives as anti-inflammatory and analgesic agents. Eur J Med Chem. 2010;45(6):2245-9.
21. Shingalapur RV, Hosamani KM, Keri RS, et al. Derivatives of benzimidazole pharmacophore: synthesis, anticonvulsant, antidiabetic and DNA cleavage studies. Eur J Med Chem. 2010;45(5):1753-9.
22. Nakano H, Inoue T, Kawasaki N, et al. Synthesis of benzimidazole derivatives as antiallergic agents with 5-lipoxygenase inhibiting action. Chem Pharm Bull (Tokyo). 1999;47(11):1573-8.
23. Apohan E, Yilmaz U, Yilmaz O, et al. Synthesis, cytotoxic and antimicrobial activities of novel cobalt and zinc complexes of benzimidazole derivatives. J Organomet Chem. 2017;828:52-8.
24. Gurer-Orhan H, Orhan H, Suzen S, et al. Synthesis and evaluation of in vitro antioxidant capacities of some benzimidazole derivatives. J Enzyme Inhib Med Chem. 2006;21(2):241-7.
25. Kerimov I, Ayhan-Kilcigil G, Can-Eke B, et al. Synthesis, antifungal and antioxidant screening of some novel benzimidazole derivatives. J Enzyme Inhib Med Chem. 2007;22(6):696-701.
26. Walter P, Ron D. The unfolded protein response: from stress pathway to homeostatic regulation. Science. 2011;334(6059):1081-6.
27. Zhang L, Wang Y. Tauroursodeoxycholic Acid Alleviates H_2O_2-Induced Oxidative Stress and Apoptosis via Suppressing Endoplasmic Reticulum Stress in Neonatal Rat Cardiomyocytes. Dose Response. 2018;16(3):1559325818782631.
28. Patil C, Walter P. Intracellular signaling from the endoplasmic reticulum to the nucleus: the unfolded protein response in yeast and mammals. Curr Opin Cell Biol. 2001;13(3):349-55.
29. Ruggiano A, Foresti O, Carvalho P. Quality control: ER-associated degradation: protein quality control and beyond. J Cell Biol. 2014;204(6):869-79.
30. Lee AH, Iwakoshi NN, Glimcher LH. XBP-1 regulates a subset of endoplasmic reticulum resident chaperone genes in the unfolded protein response. Mol Cell Biol. 2003;23(21):7448-59.
31. Lin JH, Li H, Yasumura D, et al. IRE1 signaling affects cell fate during the unfolded protein response. Science. 2007;318(5852):944-9.
32. Ge Y, Jiao Y, Li P, et al. Coregulation of endoplasmic reticulum stress and oxidative stress in neuropathic pain and disinhibition of the spinal nociceptive circuitry. Pain. 2018;159(5):894-906.
33. Cullinan SB, Diehl JA. PERK-dependent activation of Nrf2 contributes to redox homeostasis and cell survival following endoplasmic reticulum stress. J Biol Chem. 2004;279(19):20108-17.
34. Koritzinsky M, Magagnin MG, van den Beucken T, et al. Gene expression during acute and prolonged hypoxia is regulated by distinct mechanisms of translational control. EMBO J. 2006;25(5):1114-25.
35. Jung EJ, Avliyakulov NK, Boontheung P, et al. Pro-oxidative DEP chemicals induce heat shock proteins and an unfolding protein response in a bronchial epithelial cell line as determined by DIGE analysis. Proteomics. 2007;7(21):3906-18.
36. Yu G, Zeng X, Wang H, et al. 14,15-epoxyeicosatrienoic Acid suppresses cigarette smoke extract-induced apoptosis in lung epithelial cells by inhibiting endoplasmic reticulum stress. Cell Physiol Biochem. 2015;36(2):474-86.
37. Kenche H, Baty CJ, Vedagiri K, et al. Cigarette smoking affects oxidative protein folding in endoplasmic reticulum by modifying protein disulfide isomerase. FASEB J. 2013;27(3):965-77.
38. Geraghty P, Wallace A, D'Armiento JM. Induction of the unfolded protein response by cigarette smoke is primarily an activating transcription factor 4-C/EBP homologous protein mediated process. Int J Chron Obstruct Pulmon Dis. 2011;6:309-19.
39. Korfei M, Ruppert C, Mahavadi P, et al. Epithelial endoplasmic reticulum stress and apoptosis in sporadic idiopathic pulmonary fibrosis. Am J Respir Crit Care Med. 2008;178(8):838-46.